JOURNAL OF Applied Polymer SCIENCE

# Antifouling Microfiltration Membranes Prepared from Poly(vinylidene fluoride)-*graft*-Poly(*N*-vinyl pyrrolidone) Powders Synthesized via Pre-Irradiation Induced Graft Polymerization

**Lifang Chen,[1,2] Zhengchi Hou,[1] Xiaofeng Lu,[1] Peng Chen,[1,2] Zhongying Liu,[1] Liguo Shen,[1,2] Xiaokai Bian,[1,2] Qiang Qin[1,2]**

[1]Shanghai Institute of Applied Physics, Chinese Academy of Sciences, 201800 Shanghai, People's Republic of China
[2]Graduate University of Chinese Academy of Sciences, 100049 Beijing, People's Republic of China
Correspondence to: Z. Hou (E-mail: houzhengchi@sinap.ac.cn)

**ABSTRACT:** Poly(vinylidene fluoride) (PVDF) powders were grafted with *N*-vinyl pyrrolidone using the pre-irradiation induced graft polymerization technique. The effects of reaction time, absorbed dose, and monomer concentration on the degree of grafting were investigated, and the grafted PVDF powders were characterized by Fourier transform infrared spectroscopy, thermogravimetric analysis, and differential scanning calorimetry. The grafted PVDF powders were also cast into microfiltration (MF) membranes via the phase-inversion method. The contact angle and water uptake were measured. The membrane morphology was studied by scanning electron microscopy, and the water filtration properties of the membranes were tested. The antifouling properties were determined through measurements of the recovery percentage of pure water flux after the MF membranes were fouled with bovine serum albumin solution. The results confirmed that the existence of poly(*N*-vinyl pyrrolidone) (PVP) graft chains improved the hydrophilicity and antifouling properties of the MF membranes cast from PVDF-*g*-PVP powders. © 2012 Wiley Periodicals, Inc. J. Appl. Polym. Sci. 128: 3949–3956, 2013

**KEYWORDS:** irradiation; grafting; PVDF; NVP; membrane

Received 13 July 2012; accepted 21 September 2012; published online 16 October 2012
**DOI: 10.1002/app.38625**

## INTRODUCTION

Poly(vinylidene fluoride) (PVDF) is a linear semicrystalline fluoropolymer that possesses good mechanical properties, chemical stability, high temperature resistance, and numerous other merits.[1–3] It is an ideal membrane material that can be dissolved in common organic solvents, such as dimethylformamide (DMF), dimethylacetamide (DMAC), and *N*-methyl pyrrolidone (NMP), and then cast into membranes using the phase-inversion method.[4,5] Furthermore, it has been widely used in environmental protection, water treatment, petrochemical processing, food processing, etc. Because of its hydrophobicity, PVDF can easily adsorb proteins and many other large molecules during the membrane separation process, resulting in membrane fouling, which, in turn, restricts the applications of PVDF membranes. In general, better hydrophilicity favors improvement in antifouling property, therefore, increasing the hydrophilicity of PVDF is particularly important.[6–8] In recent years, researchers have attempted to graft hydrophilic monomers into PVDF main chains or onto PVDF membrane surfaces. Grafting methods, such as surface living/controlled radical polymerization,[7,9,10] the plasma-induced grafting method,[11–13] UV-assisted graft polymerization,[14,15] and radiation-induced graft polymerization, are often employed. The radiation-induced graft polymerization has attracted significant attention because of its mild reaction temperature and ease of operation.

A well-known method for modifying polymers' physical and chemical properties, radiation-induced graft polymerization involves two main methods: (1) simultaneous irradiation method and (2) pre-irradiation method, which has been extensively used to modify polymers' properties because it results in little homopolymer formation and the grafting can be performed away from the irradiation source, which is favorable for mass production.[2,16,17]

Many hydrophilic monomers, including acrylic acid, acrylamide, and methyl methacrylate, have been grafted onto PVDF membrane surfaces or into PVDF main chains. In our work, the grafting of these monomers was found to have some influence on the solubility of PVDF, which is not beneficial to membrane preparation. However, the graft polymerization of *N*-vinyl pyrrolidone (NVP) onto PVDF powders has very little effect on the solubility of PVDF under our experimental conditions.

Furthermore, poly(vinyl pyrrolidone) (PVP), the polymer of NVP, has excellent hydrophilicity, chemical stability, complexing capacity, and biocompatibility. It has broad application prospects in the field of biology, medicine, materials, etc. Numerous studies have concentrated on the modification of polymers using NVP as a monomer.[18–22] Chen and Belfort[19] have studied the surface modification of poly(ether sulfone) (PES) ultrafiltration membranes by low-temperature plasma-induced graft polymerization. Their results showed that the surface-modified membranes were notably less susceptible to bovine serum albumin (BSA) fouling than the virgin PES membrane or a commercial low-protein binding PES membrane. In addition, the modified membranes were easier to clean and required treatment with little caustic to recover the permeation flux. Zhang et al.[22] have reported that the PVDF membrane modification by surface grafting of hydrophilic PVP chains can effectively prevent the membrane from protein adsorption in static experiments, and the membrane fouling during filtration. When adsorption occurred on the modified membrane surface, the adsorbed proteins could be more easily removed by pure water or by mild cleaning with a dilute alkaline solution, in comparison with the unmodified membrane.

In the present work, NVP was grafted onto PVDF powders by pre-irradiation induced graft polymerization and then the microfiltration (MF) membranes were cast from PVDF-*g*-PVP powders with different degrees of grafting (DG) via the phase-inversion method. The kinetics of the graft polymerization was studied and the grafted PVDF powders were characterized by Fourier transform infrared (FTIR) spectroscopy, thermogravimetric analysis (TGA), and differential scanning calorimetry (DSC). The hydrophilicity, morphology, and filtration properties of the modified MF membranes were investigated. The antifouling properties were studied using BSA as a model contaminator.

## EXPERIMENTAL

### Materials

PVDF powders (TA-6020) were purchased from Solvay Co. (Brussels, Belgium). NVP was obtained from J&K Corporation (Shanghai, China). DMF, $FeSO_4(NH_4)_2SO_4{\cdot}6H_2O$, NMP, HCl, phosphate-buffered saline (PBS), and poly(ethylene glycol) (PEG-400) were purchased from Sinopharm Reagent Co. (Shanghai, China). BSA ($M_w$ = 67,000) was purchased from Shanghai Bio Life Science and Technol. Co. (Shanghai, China). PE non-woven fabric (TYVEK 1057 D) was obtained from DuPont Co. (USA). PVDF powders were washed with deionized water to remove impurities, and then dried in vacuum at 70°C until a constant weight was obtained. Distilled water was used to prepare the monomer solution. The other mentioned materials were used without further purification.

### Pre-Irradiation Induced Graft Polymerization

The purified PVDF powders were irradiated in the air using a $^{60}Co$ gamma source at room temperature. The dose range was from 5 kGy to 30 kGy, and the dose rate was 0.294 kGy/h. After irradiation, the PVDF powders were stored at −24°C in a refrigerator before use. NVP concentrations from 5% to 50% were prepared by adding the monomer to water in a 250-mL Erlenmeyer flask. The inhibitor ($FeSO_4(NH_4)_2SO_4{\cdot}6H_2O$, 0.1961 g) and 20 g of irradiated PVDF powders were added to the flask, and the mixture was bubbled with nitrogen gas for 15 min to remove oxygen. The flask was subsequently sealed, and the graft polymerization was performed at 70°C under stirring for a defined time. After the reaction, the grafted PVDF powders were filtered. They were then washed twice with 1*M* HCl solution at 60°C while stirring for 2 h to remove the metal ions. The powders were subsequently washed with water three times. Finally, the PVDF-*g*-PVP powders were dried at 70°C in vacuum to a constant weight.

DGs of the PVDF-*g*-PVP powders were determined by fluorine elemental analysis.[23,24]

### Powder Characterization

The FTIR spectra were recorded on a Nicolet Avatar 370 FTIR spectrometer (Thermo Nicolet Instrument Corporation, WI, USA) in the transmission mode, and 32 scans were accumulated at a resolution of 4 $cm^{-1}$; the pristine and grafted PVDF powders were pressed into pellets with KBr before measurements.

The thermal decomposition behavior of the pristine and grafted PVDF powders was investigated by TGA, which was performed under a nitrogen atmosphere with a NETZSCH 209 F3 Tarsus TG (NETZSCH Instruments Manufacturing Co., Germany) in the range of 20–800°C at a heating rate of 10 °C/min. Before the tests, the samples were dried in vacuum at 70°C for 24 h.

DSC was conducted on a METTLER TOLEDO DSC822e DSC instrument (Mettler-Toledo International, Zurich, Switzerland) in the temperature range 25–250°C and at a heating rate of 10 °C/min under a nitrogen gas atmosphere. The measurements were performed on samples that weighted approximately 10 mg using an aluminum crucible. To eliminate the thermal history of the powders, scans were taken twice with the same scan parameters, and the second scan results were recorded.

### Microfiltration Membrane Preparation

**MF Membranes were Prepared by the Phase-Inversion Method as Follows.** Pristine or grafted PVDF powders and the pore-forming agent (PEG-400) were dissolved in NMP at 70°C with a weight ratio of 8 : 1.5 : 40.5 for 7 days. The solution was cast onto non-woven fabric taped on a glass plate at (27 ± 1)°C, which was then immersed in a precipitation bath of deionized water maintained at (18 ± 1)°C after the new-born membrane had been evaporated in air for 20 s. For all of the prepared membranes, after complete precipitation, the membrane was transferred to a drip-washing water bath for 3 days at room temperature to remove residual solvent. The prepared membranes were stored in fresh deionized water before further characterization.

### Membrane Characterization

**Contact Angle Measurements.** Contact angles of the dense membranes, which were cast from PVDF or grafted PVDF solutions (in DMF) by spin-coating, were measured at room temperature on an Attension Theta System (KSV Instruments, Finland). Five microliters of deionized water was dropped onto the membrane surface from a needle tip; the contact angle was

determined with computation software. The contact angle value of a membrane was averaged from tests at five different points.

**Scanning Electron Microscopy.** The morphology of the MF membranes was measured using a LEO1530vp scanning electron microscopy (SEM, Zeiss, Germany). Samples were attached by carbon tape to the sample stage and sputtered with gold prior to the SEM measurements. The voltage was set at 25 kV, and the current was set at 10 mA. To obtain the cross-section images, membranes were fractured using liquid nitrogen before measurements.

**Water Uptake Measurements.** MF membranes were rinsed with deionized water, and then dried in a vacuum oven at 60°C for 24 h. The dried membranes were subsequently immersed in deionized water for at least 24 h. The swollen membranes were then taken out from the water, and the surface of the membrane was quickly wiped with filtration paper to remove excess water adhered to the surface; the membranes were then immediately weighed ($W_s$) before the membranes were dried under vacuum at 60°C for 24 h. The dried membranes were quickly measured ($W_d$), and the water uptake was calculated using the following equation:

$$\text{Water uptake}\ (\%) = \frac{W_s - W_d}{W_d} \times 100 \quad (1)$$

where $W_s$ and $W_d$ are the weight of the swollen and dry MF membranes, respectively.

**Flux Measurements.** The filtration properties were characterized by measuring the flux of the MF membranes on a MF cell apparatus.[25] The sample membranes were immersed in deionized water overnight before measurement. A membrane was mounted onto the MF cell with a valid area of 0.002 $m^2$ and pre-compacted at −10 kPa for a certain time until the flux maintained a constant value. The flux ($J$) was calculated according to eq. (2):

$$J = \frac{V}{A \times \Delta T} \quad (2)$$

where $V$ is the volume of the permeation water, $A$ is the effective area of the membrane, and $\Delta T$ is the time of the measurement.

**Characterization of Antifouling Properties.** The antifouling properties of the MF membranes were evaluated by measuring the percentage of water flux recovery after fouling by BSA solution. After the water flux measurement, pure water was changed to 1 g/L BSA solution in PBS (pH = 7.4). The sample membrane was kept filtering for 2 h with protein solution under stirring; later, the fouling membrane was flushed with deionized water, and the recovered water flux, $J_1$, was measured again.

The flux recovery percentage ($R$) is calculated according to eq. (3):

$$R(\%) = \frac{J_1}{J_0} \times 100 \quad (3)$$

where $J_0$ is the pure water flux of the sample membrane before fouling and $J_1$ is the pure water flux after fouling.

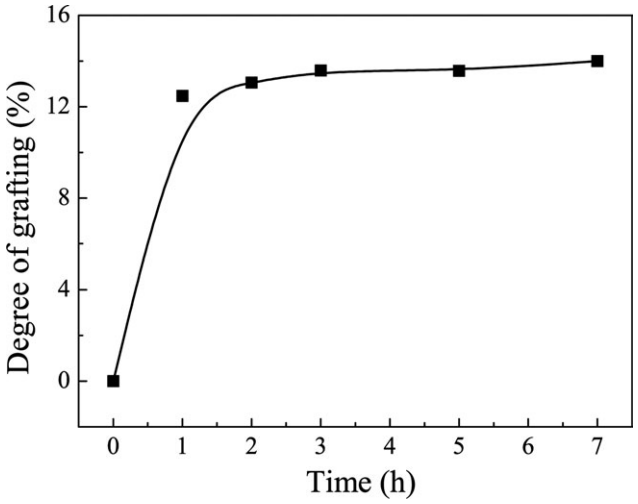


**Figure 1.** Effect of reaction time on the grafting of NVP for 20 kGy irradiated PVDF at 70°C. The corresponding concentrations of monomer and inhibitor were 10% and 5 mmol/L, respectively.

## RESULTS AND DISCUSSION

### Graft Polymerization Kinetics Study

In the pre-irradiation induced graft polymerization process, PVDF powders are first irradiated in air to form peroxides. Heating is required to decompose the stable peroxides into radicals, which initiate the graft polymerization. The temperature was controlled at 70°C, a normal temperature for decomposing peroxides. In order to suppress homopolymerization, which is less likely than in simultaneous irradiation, Mohr's salt of 5 mmol/L was added. The main parameters of DG, i.e., the reaction time, absorbed dose, and monomer concentration were varied in this investigation to obtain the regularities of graft polymerization of NVP onto PVDF powders.

**Influence of Reaction Time.** Figure 1 shows the effect of reaction time on the grafting process. The grafting showed an initial increase and then reached saturation with increased time. At the beginning of the grafting, the monomer concentration and the free radical concentration are relatively high in the reaction system; therefore, DG increases rapidly. However, the monomer and free radicals are consumed with increasing time; consequently, the grafting is terminated gradually.

**Influence of Absorbed Dose.** Figure 2 presents the effect of absorbed dose on the grafting process. As evident in the figure, DG increased with increasing absorbed dose, and grafting saturation was achieved when absorbed dose exceeded 10 kGy. The irradiation of PVDF in the air leads to the formation of peroxides, which act as the grafting initiator in polymerization. With the increasing absorbed dose, the amount of peroxides increases, which results in a higher DG. The grafting saturation at higher doses (>10 kGy) can be ascribed to the recombination of primary radicals and decomposition of the peroxides.[26]

**Influence of Monomer Concentration.** Figure 3 shows the effect of monomer concentration on the grafting process. As clearly shown in this figure, DG increased with increasing

Applied Polymer SCIENCE

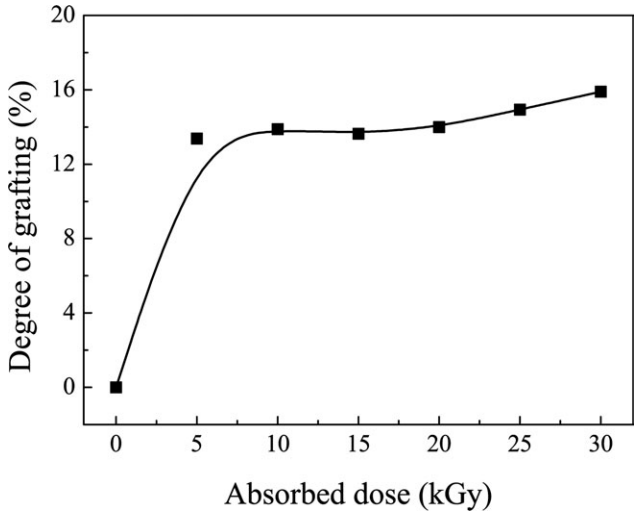


**Figure 2.** Effect of absorbed dose on the grafting of NVP for irradiated PVDF at 70°C. The reaction time was 5 h, and the corresponding concentrations of monomer and inhibitor were 10% and 5 mmol/L, respectively.

monomer concentration when the concentration was less than 20% before leveling off. This is attributed to the increase in NVP molecules available close to grafting sites. The pre-irradiation grafting is usually controlled to a large extent by diffusion of the monomer to grafting sites, in which case grafting starts at the surface of the PVDF powders and proceeds internally by a continuous diffusion of NVP through the already grafted layer, until an equilibrium swelling of the grafted layer is reached at a certain monomer concentration. The reason for leveling off is two-fold. On the one hand, at high monomer concentrations, the graft reaction is dominated by diffusion into polymers. On the other, the number of grafting sites where reaction takes place at a certain dose is constant regardless of the increase in monomer concentration.[2,27]

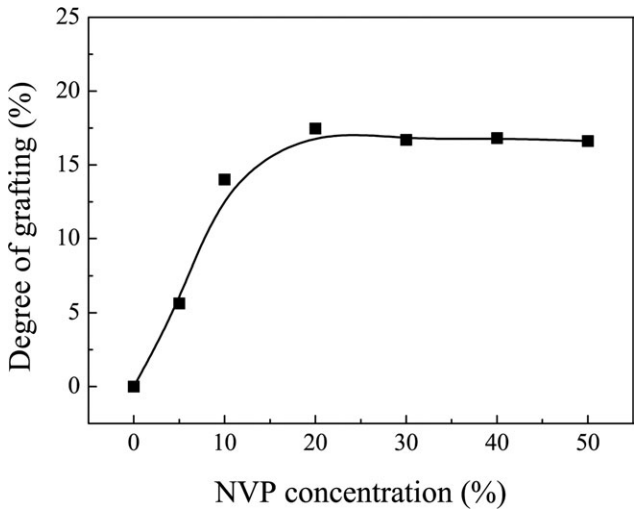


**Figure 3.** Effect of monomer concentration on the grafting of NVP for 20 kGy irradiated PVDF at 70°C. The reaction time was 5 h, and the inhibitor concentration was 5 mmol/L.

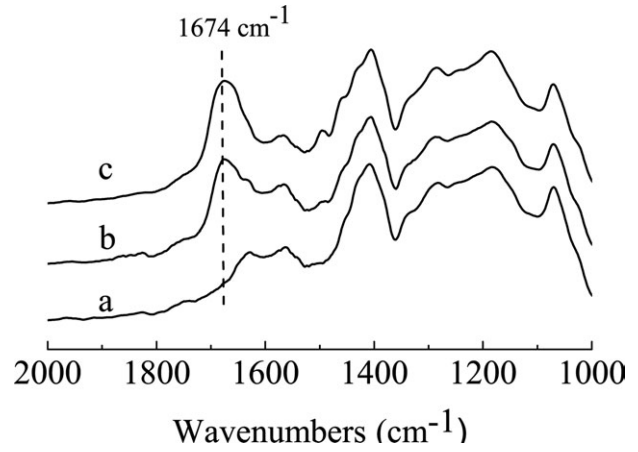


**Figure 4.** FTIR spectra of (a) pristine PVDF powders and PVDF-*g*-PVP powders with DGs of (b) 6.31% and (c) 14.69%.

## Powder Characterization

**FTIR Spectroscopy.** FTIR spectra of pristine and grafted PVDF powders with different DGs are compared in Figure 4. In the spectrum of the pristine PVDF powders, the absorption band at 1632 $cm^{-1}$ is ascribed to the stretching vibrations of C=C bond. Notably, a new distinctive band at 1674 $cm^{-1}$ appeared after grafting with NVP, which is due to C=O stretching vibrations in the PVP chains. The increase in the absorbance of this band with increasing DG indicates that NVP monomers have been successfully grafted onto PVDF.

**Thermal Properties.** The TGA profiles of pristine, irradiated, and grafted PVDF powders are shown in Figure 5. As can be seen from Figure 5, the TGA curve of the PVDF powders irradiated with 5 kGy $\gamma$-ray did not change significantly compared to the curve of pristine PVDF, which indicates that the 5 kGy dose of $\gamma$-ray irradiation did not change the thermal stability of PVDF. The TGA of pristine PVDF showed one major weight loss, whereas the TGA of PVDF-*g*-PVP exhibiting a two-step weight loss, which began at approximately 340°C and continued until 460°C, is due to the decomposition of PVP; the second

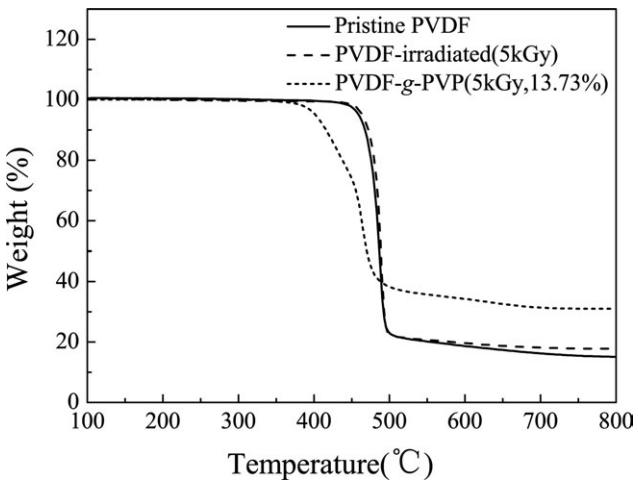


**Figure 5.** TGA of the pristine PVDF, irradiated PVDF (5 kGy), and grafted PVDF powders with a DG of 13.73%.

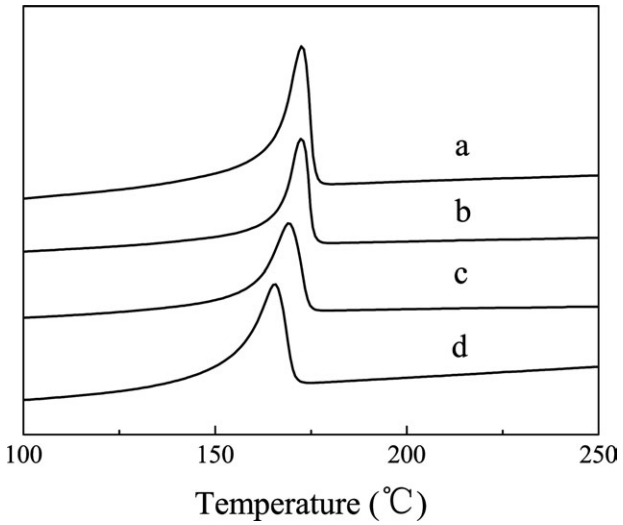


**Figure 6.** DSC curves of (a) pristine PVDF, (b) irradiated PVDF (20 kGy), and grafted PVDF powders with DGs of (c) 13.92% and (d) 16.85%.

weight loss, starting at approximately 460°C, is attributed to the decomposition of the base material PVDF. The TGA curves also showed that the residue weight of PVDF-*g*-PVP was much more than that of the pristine PVDF. This might be because PVDF-*g*-PVP tends to generate less volatile substances than PVDF does. Similar results have been reported by Xu et al.[28] The difference in the weight loss pattern in the case of grafted and pristine PVDF powders is evident in Figure 5, which further confirms the grafting of PVDF with NVP. Furthermore, the two-step decomposition suggests that the PVP grafts do not alter the inherent decomposition of the matrix PVDF.

Figure 6 shows the calorimetric curves of pristine, irradiated (20 kGy), and some grafted PVDF samples. The melting temperature ($T_m$), melting enthalpy ($\Delta H_m$), and degree of crystallinity of these samples are listed in Table I.

The DSC curves show the calorimetric curve of PVDF did not change after irradiation at 20 kGy, which indicates that PVDF has certain radiation stability. This result is in agreement with the data reported by Calcagno et al.[29] However, after grafting, the melting peak became broader, and its melting temperature shifted to lower values with increasing DG.

The degree of crystallinity was evaluated through eq. (4), where $\Delta H_m$ is the melting enthalpy of the material under study and

**Table I.** Melting Temperature ($T_m$), Melting Enthalpy ($\Delta H_m$) and Degree of Crystallinity of Pristine, Irradiated and Grafted Samples

| Sample | DG (%) | $T_m$ (°C) | $\Delta H_m$ (J/g) | Degree of crystallinity (%) |
|---|---|---|---|---|
| Pristine PVDF | – | 172.66 | 51.59 | 49.32 |
| Irradiated PVDF | – | 172.34 | 48.70 | 46.56 |
| PVDF-*g*-PVP | 13.92% | 169.14 | 43.32 | 41.41 |
| PVDF-*g*-PVP | 16.85% | 165.49 | 33.23 | 31.77 |

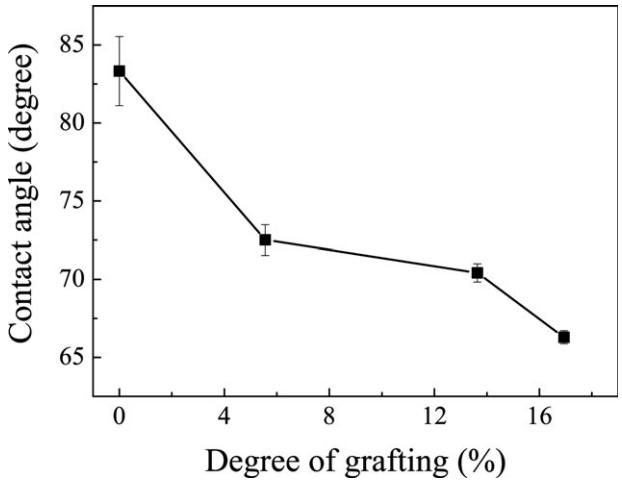


**Figure 7.** The relationship between the water contact angle and DG of dense membranes cast from pristine PVDF and PVDF-*g*-PVP powders.

$\Delta H_0$ is the melting enthalpy of the totally crystalline material. For PVDF, $\Delta H_0 = 104.6$ J/g.[30,31]

$$\text{Degree of crystallinity } (\%) = \frac{\Delta H_m}{\Delta H_0} \times 100 \qquad (4)$$

As shown in Table I, PVDF is semicrystalline. Moreover, the melting enthalpy and the degree of crystallinity of PVDF after grafting decreased with increasing DG, which is attributed to the presence of amorphous PVP. A similar phenomenon was observed in the process of grafting styrene onto PVDF film induced by high energy ions.[32]

**Membrane Characterization**

**Contact Angle Measurements.** As shown in Figure 7, the contact angle of modified membranes cast from PVDF-*g*-PVP powders was lower than that of the pristine membrane, which is attributed to the hydrophilicity of carbonyl groups in the PVP chains. The water contact angle of dense membranes decreased from 83.33° to 66.29° when DG was increased to 16.94%. Based on these results, it can be inferred that the hydrophilic PVDF can be obtained by grafting with NVP.

**Morphology of the MF Membranes.** The surface and cross-section SEM images of the MF membranes cast from pristine PVDF and PVDF-*g*-PVP powders are shown in Figure 8. A comparison of the surface images [Figure 8(a1,b1)] reveals that the number of pores in the MF membranes cast from PVDF-*g*-PVP powders (DG = 5.56%) was evidently greater than that in the pristine membrane. In addition, the pore sizes were larger than those in the pristine sample. However, the number of pores and pore sizes decreased when DG was increased to 16.94% [Figure 8(b1,c1)].This is due to the increase in the number of PVP chains, which intertwine with each other or with the pore-forming agent (PEG) and hamper the diffusion of PEG into water during the membrane formation. Furthermore, the swell of the hydrophilic PVP during the soaking process also results in a reduction in pore size.[22,33] Similar results have been reported by Yang et al.,[34] who grafted poly(*N*,*N*-dimethylacrylamide) onto PVDF powders. As evident from the cross-section SEM images,

Applied Polymer SCIENCE

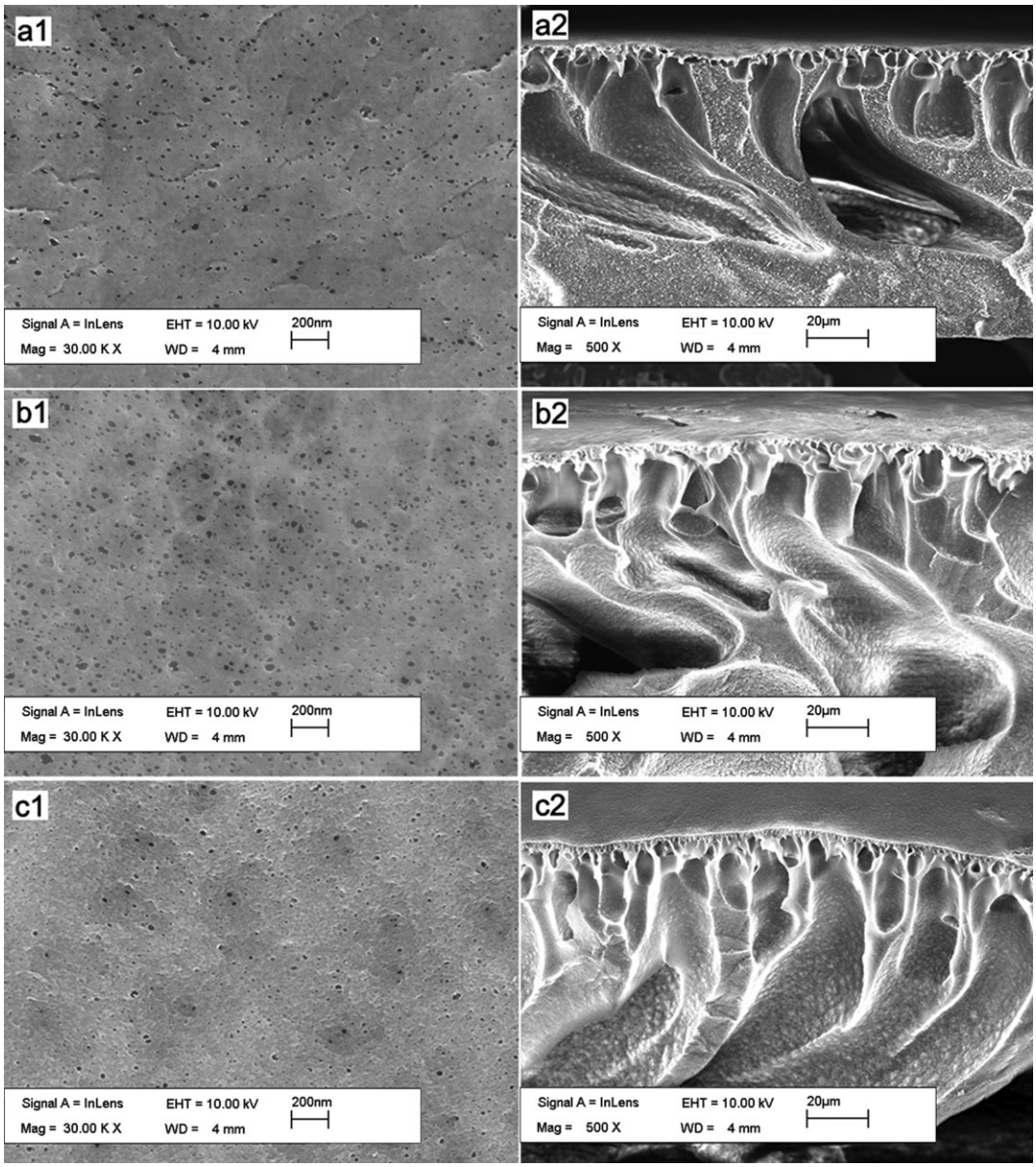


**Figure 8.** Surface (left) and cross-section (right) SEM images of the MF membranes cast from (a) pristine PVDF powders and PVDF-*g*-PVP powders with DGs of (b) 5.56% and (c) 16.94%.

an asymmetric morphology with a skin layer as a selective barrier and macrovoids in the support layer was observed for these MF membranes. What's more, there was a small change in thickness after modification. This change may due to a variable exchange rate between water and the solvent.[35] In addition, the different angles from which the SEM images were taken may also have caused the differences in thickness.

**Water Uptake Measurements.** As evident from the results in Figure 9, the water uptake of the modified membranes was greater than that of the pristine PVDF membrane; in addition, the water uptake of the modified membrane with a DG of 16.94% was less than that of the membrane with a DG of 5.56%. Hydrophilicity, pore amount, and size all are known to affect the water uptake.[36,37] The hydrophilicity of a membrane material is enhanced with increasing DG, which favors the water uptake, whereas the pore amount and size of the modified membrane with a DG of 16.94% are less than those of the membrane with a DG of 5.56%, which can be observed in the surface SEM images. Therefore, the finding that the water uptake of the modified membrane with a DG of 5.56% is greater than that of the membrane with a DG of 16.94% can be explained by the combined contribution of these factors.

**Flux of MF Membranes.** Figure 10 presents the flux test results of the pristine PVDF and modified PVDF membranes. Similar to the results of the water uptake tests mentioned in the previous section, the flux of the modified MF membranes were higher than that of the pristine PVDF membrane, and the MF membrane with a DG of 5.56% exhibited the highest flux,

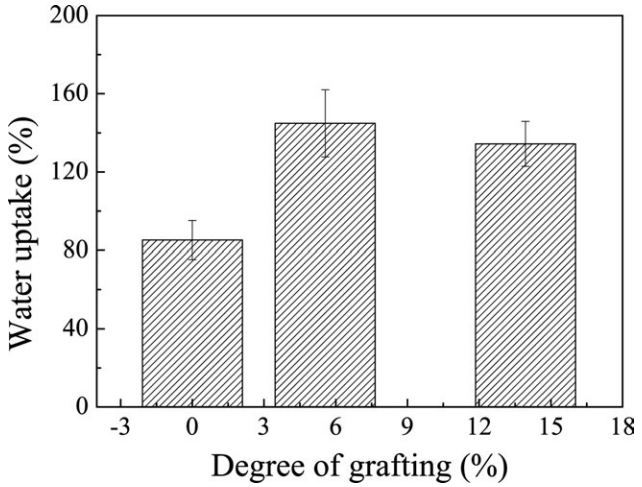


**Figure 9.** Water uptake of MF membranes cast from pristine PVDF and PVDF-*g*-PVP powders at different DGs.

which was three times higher than that of the pristine membrane. Improved hydrophilicity, a greater number of pores, and a larger pore size are beneficial to the improvement in flux.[25] Although the MF membrane with a DG of 16.94% showed the highest hydrophilicity based on the contact angle results, the surface SEM images showed that the number of pores and their size were less than those of the membrane with a DG of 5.56%, which can be attributed to the higher extent of swell and cross-link resulted from more hydrophilic PVP at a higher DG. Considering these two factors, the flux of the modified membrane with a DG of 16.94% was less than that of the membrane with a DG of 5.56%.

**Antifouling Properties of MF Membranes.** The effect of grafting on the antifouling behavior of the MF membranes was investigated with respect to dynamic BSA fouling. The results in terms of permeate flux relative to pure water flux are depicted in Figure 11. It can be seen that the modified membranes demonstrated the higher permeation flux than that of the pristine

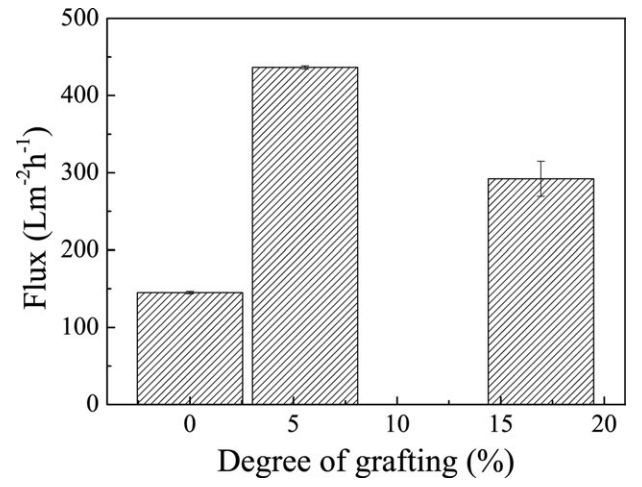


**Figure 10.** Flux of MF membranes cast from pristine PVDF and PVDF-*g*-PVP powders at different DGs.

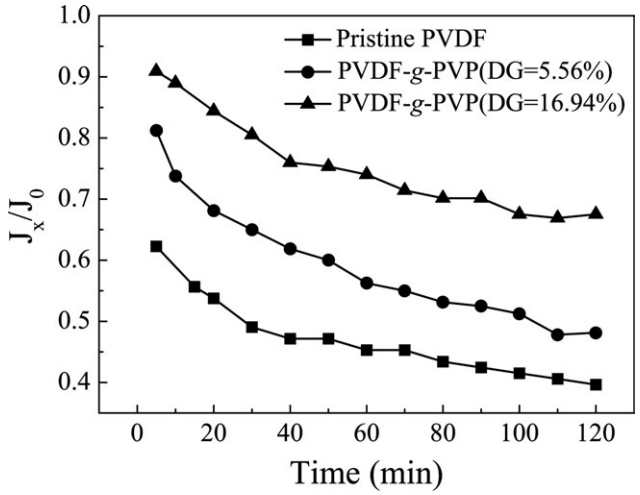


**Figure 11.** Normalized flux of MF membranes cast from pristine PVDF and PVDF-*g*-PVP powders at different DGs during filtration of 1 g/L BSA solution.

PVDF membrane, which was mainly influenced by BSA fouling. Overall, the final permeation flux of BSA for the modified membrane (DG = 16.94%) was 62% of the initial permeation flux.

As shown in Figure 12, the flux recovery percentage of these MF membranes cast from the PVDF-*g*-PVP powders were greater than that of the membrane cast from the pristine PVDF powders, which indicates the better antifouling properties of the MF membranes cast from PVDF-*g*-PVP powders. In addition, with the elevated DG, the water recovery percentage of the MF membranes cast from PVDF-*g*-PVP powders increased.

As is well known, hydrophilic membranes mitigate protein adsorption due to the repulsion force from the hydrated layers on the surface. PVP is an electrically neutral hydrophilic polymer that, in the presence of water, immobilizes water molecules

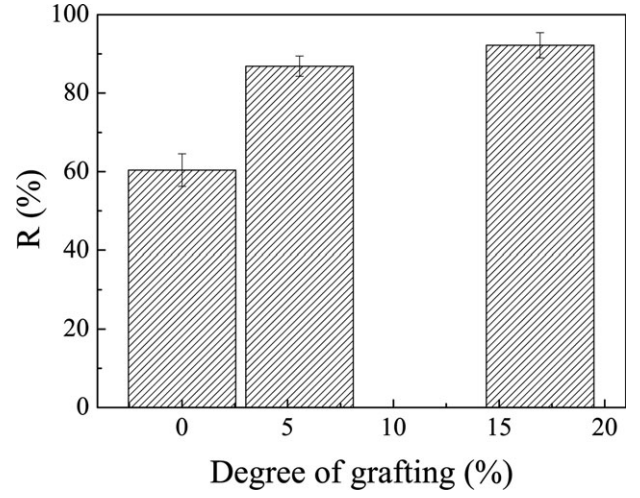


**Figure 12.** Water flux recovery percentage of MF membranes cast from pristine PVDF and PVDF-*g*-PVP powders at different DGs after 2 h of fouling with BSA solution.

in the vicinity of the amide group. Therefore, the water is bound to the grafted PVP chains and mitigates protein adsorption on the membrane surface by repulsion of hydrated layers.[38]

## CONCLUSIONS

PVDF powders were grafted with NVP using the pre-irradiation induced graft polymerization method. The existence of PVP grafts in PVDF powders was demonstrated by FTIR spectroscopy measurements. The DG of NVP increased with increasing reaction time, absorbed dose, and monomer concentration, with a maximum value of around 20%. The melting temperature, the degree of crystallinity, and the thermal stability of the PVDF powders decreased after grafting.

MF membranes were cast from pristine PVDF and PVDF-*g*-PVP powders with different DGs using the phase-inversion method. The contact angle results showed that the hydrophilicity of the membrane material increased with increasing DG, which led to a reduced contact angle. The morphology study suggested that the modified membrane with a DG of 5.56% exhibited the greatest number of pores and the largest pore size, which led to the highest water uptake and water flux among the investigated membranes. The modified membranes exhibited better antifouling properties because of the enhanced hydrophilicity, and the modified membrane with a DG of 16.94% exhibited the best antifouling property.

## ACKNOWLEDGMENTS

This study was supported by National Natural Science Foundation of China (20776147) and by Shanghai Commission for Science and Technology (08231200300).

## REFERENCES

1. Forsythe, J. S.; Hill, D. J. T. *Prog. Polym. Sci.* **2000**, *25*, 101.
2. Dargaville, T. R.; George, G. A.; Hill, D. J. T.; Whittaker, A. K. *Prog. Polym. Sci.* **2003**, *28*, 1355.
3. Betz, N.; Begue, J.; Goncalves, M.; Gionnet, K.; Deleris, G.; Moel, A. L. *Nucl. Instrum. Methods Phys. Res. B* **2003**, *208*, 434.
4. Ulbricht, M. *Polymer* **2006**, *47*, 2217.
5. Yeow, M. L.; Liu, Y. T.; Li, K. *J. Appl. Polym. Sci.* **2004**, *92*, 1782.
6. Ying, L.; Kang, E. T.; Neoh, K. G. *J. Membr. Sci.* **2002**, *208*, 361.
7. Zhai, G. Q.; Kang, E. T.; Neoh, K. G. *Macromolecules* **2004**, *37*, 7240.
8. Chang, Y.; Shih, Y. J.; Ruaan, R. C.; Higuchi, A.; Chen, W. Y.; Lai, J. Y. *J. Membr. Sci.* **2008**, *309*, 165.
9. Singh, N.; Husson, S. M.; Zdyrko, B.; Luzinov, I. *J. Membr. Sci.* **2005**, *262*, 81.
10. Chen, Y. W.; Deng, Q.; Xiao, J. C.; Nie, H. R.; Wu, L. C.; Zhou, W. H.; Huang, B. W. *Polymer* **2007**, *48*, 7604.
11. Kaur, S.; Ma, Z. W.; Gopal, R.; Singh, G.; Ramakrishna, S.; Matsuura, T. *Langmuir* **2007**, *23*, 13085.
12. Park, Y. W.; Inagaki, N. *Polymer* **2003**, *44*, 1569.
13. Duca, M. D.; Plosceanu, C. L.; Pop, T. *Polym. Degrad. Stab.* **1998**, *61*, 65.
14. Taniguchi, M.; Belfort, G. *J. Membr. Sci.* **2004**, *231*, 147.
15. Rahimpour, A.; Madaeni, S. S.; Zereshki, S.; Mansourpanah, Y. *Appl. Surf. Sci.* **2009**, *255*, 7455.
16. Nasef, M. M.; Hegazy, E. S. A. *Prog. Polym. Sci.* **2004**, *29*, 499.
17. Aydinli, B.; Tincer, T. *Radiat. Phys. Chem.* **2001**, *60*, 237.
18. Pieracci, J.; Crivello, J. V.; Belfort, G. *Chem. Mater.* **2002**, *14*, 256.
19. Chen, H.; Belfort, G. *J. Appl. Polym. Sci.* **1999**, *72*, 1699.
20. Chen, K. S.; Ku, Y. A.; Lin, H. R.; Yan, T. R.; Sheu, D. C.; Chen, T. M. *J. Appl. Polym. Sci.* **2006**, *100*, 803.
21. Liu, Z. M.; Xu, Z. K.; Wang, J. Q.; Wu, J.; Fu, J. *J. Eur. Polym. J.* **2004**, *140*, 2077.
22. Zhang, M.; Nguyen, Q. T.; Ping, Z. *J. Membr. Sci.* **2009**, *327*, 78.
23. Geng, W. H.; Nakajima, T.; Takanashi, H.; Ohki, A. *Fuel* **2007**, *86*, 715.
24. Yu, M.; Zhang, B. W.; Deng, B.; Yang, X. X.; Sheng, K. L.; Xie, L. D.; Lu, X. F.; Li, J. Y. *J. Appl. Polym. Sci.* **2010**, *117*, 3575.
25. Deng, B.; Yang, X. X.; Xie, L. D.; Li, J. Y.; Hou, Z. C.; Yao, S. D.; Liang, G. M.; Sheng, K. L.; Huang, Q. *J. Membr. Sci.* **2009**, *330*, 363.
26. Ikram, S.; Kumari, M.; Gupta, B. *Radiat. Phys. Chem.* **2011**, *80*, 50.
27. Nasef, M. M.; Saidi, H.; Dahlan, K. Z. M. *Radiat. Phys. Chem.* **2011**, *80*, 66.
28. Xu, C. Q.; Huang, W.; Zhou, Y. F.; Yan, D. Y.; Chen, S. T.; Huang, H. *Radiat. Phys. Chem.* **2012**, *81*, 426.
29. Calcagno, L.; Musumeci, P.; Percolla, R.; Foti, G. *Nucl. Instrum. Methods Phys. Res. B* **1994**, *96*, 461.
30. Teyssedre, G.; Bernes, A.; Lacabanne, C. *J. Polym. Sci. Part B: Polym. Phys.* **1993**, *31*, 2027.
31. Nakagawa, K.; Ishida, Y. *J. Polym. Sci. Part B: Polym. Phys. Ed.* **1973**, *11*, 1503.
32. Percolla, R.; Musumeci, P.; Calcagno, L., Foti, G.; Ciavola, G. *Nucl. Instrum. Methods Phys. Res. B* **1995**, *105*, 181.
33. Wang, D. L.; Li, K.; Teo, W. K. *J. Membr. Sci.* **1999**, *163*, 211.
34. Yang, X. X.; Zhang, B. W.; Liu, Z. Y.; Deng, B.; Yu, M.; Li, L. F.; Jiang, H. Q.; Li, J. Y. *J. Mater. Chem.* **2011**, *21*, 11908.
35. Shen, L. G.; Bian, X. K.; Lu, X. F.; Shi, L. Q.; Liu, Z. Y.; Chen, L. F.; Hou, Z. C.; Fan, K. *Desalination* **2012**, *293*, 21.
36. Liu, Q.; Song, L. Z.; Zhang, Z. H.; Liu, X. W. *Int. J. Energy Environ.* **2010**, *1*, 643.
37. Ostrovskii, D. I.; Torell, L. M.; Paronen, M.; Hietala, S.; Sundholm, F. *Solid State Ionics* **1997**, *97*,315.
38. Ping, Z. H.; Nguyen, Q. T.; Chen, S. M.; Zhou, J. Q.; Ding, Y. D. *Polymer* **2001**, *42*, 8461.